J|A|C|S
ARTICLES
Published on Web 10/03/2006

An Efficient Proton-Coupled Electron-Transfer Process during Oxidation of Ferulic Acid by Horseradish Peroxidase: Coming Full Cycle

Etienne Derat and Sason Shaik*

Contribution from the Department of Organic Chemistry and the Lise Meitner-Minerva Center for Computational Quantum Chemistry, Hebrew University of Jerusalem, Givat Ram Campus, 91904 Jerusalem, Israel

Received July 16, 2006; E-mail: sason@yfaat.ch.huji.ac.il

Abstract: Quantum mechanics/molecular mechanics calculations were utilized to study the process of oxidation of a native substrate (ferulic acid) by the active species of horseradish peroxidase (Dunford, H. B. *Heme Peroxidases*; Wiley-VCH: New York, 1999), Compound I and Compound II, and the manner by which the enzyme returns to its resting state. The results match experimental findings and reveal additional novel features. The calculations demonstrate that both oxidation processes are initiated by a proton-coupled electron-transfer (PCET) step, in which the active species of the enzyme participate *only as electron-transfer partners*, while the entire proton-transfer event is being relayed from the substrate to and from the His42 residue by a water molecule (W402). The reason for the observed (Henriksen, A; Smith, A. T.; Gajhede, M. *J. Biol. Chem.* **1999**, *274*, 35005−35011) similar reactivities of Compound I and Compound II toward ferulic acid is that the reactive isomer of Compound II is the, hitherto unobserved, $Por^{\bullet+}Fe^{III}OH$ isomer that resembles Compound I. The PCET mechanism reveals that His42 and W402 are crucial moieties and *they determine the function of the HRP enzyme* and account for its ability to perform substrate oxidation (Poulos, T. L. Peroxidases and Cytochrome P450. In *The Porphyrin Handbook*; Kadish, K. M., Smith, K. M., Guilard, R., Eds.; Academic Press: New York, 2000; Vol. 4, pp 189). In view of the results, the possibility of manipulating substrate oxidation by magnetic fields is an intriguing possibility.

Introduction

Horseradish peroxidase (HRP) is an enzyme that catalyzes the oxidative coupling of a variety of aromatic phenols by using the oxidant H_2O_2 as a cofactor.[1] While the biological function of these oxidative processes is not yet fully resolved, there is evidence that they are essential for cell wall formation and repair, including as a means of protection against viruses, fungi, etc., in the plant kingdom.[1g] For example, ferulic acid (see Scheme 1), an in vivo substrate of HRP, undergoes dimerization and cross-linking with polysugars for maintaining the robustness of the plant cell walls.[2] This oxidative coupling requires high-energy radical species that can dimerize and polymerize, and as such the process of substrate oxidation by HRP poses interesting mechanistic questions, which are addressed in this work at a molecular level using theoretical means. Let us discuss some of the questions more specifically.

The HRP enzyme uses a typical catalytic cycle with a primary active species, called Compound I (Cpd I) and shown in Scheme 1, as the high-valent oxoiron porphyrin complex **1**. Cpd I has two oxidation equivalents above the resting state, and it can therefore oxidize the organic molecule by abstracting one electron or one electron and one proton, thereby producing the secondary active species, called Compound II (Cpd II). The latter species, still being a potent oxidant, oxidizes another molecule of the organic substrate and returns to the resting state of the enzyme. Are these processes stepwise electron transfer (ET) followed by proton transfer (PT), are they coupled,[1g] i.e., proton-coupled electron-transfer (PCET) mechanisms,[3] or are they simply hydrogen atom abstraction processes? These and a host

Scheme 1. Catalytic Cycle of HRP in the Presence of Ferulic Acid with Cpd I and Cpd II Isomers (see Ref 10)

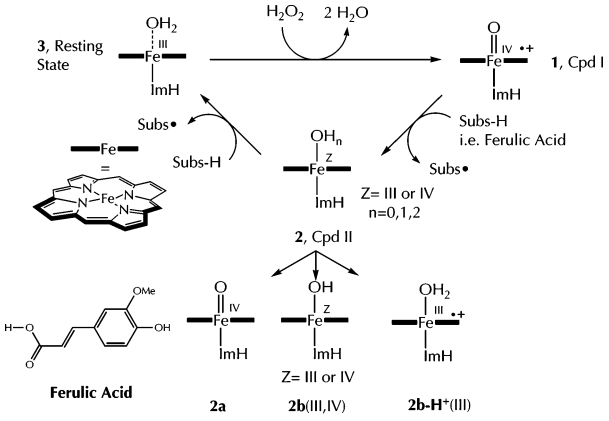

(1) (a) Meunier, B. *Chem. Rev.* **1992**, *92*, 1411−1456. (b) Poulos, T. L. Peroxidases and Cytochrome P450. In *The Porphyrin Handbook*; Kadish, K. M., Smith, K. M., Guilard, R., Eds.; Academic Press: New York, 2000; Vol. 4, Chapter 32, pp 189−218. (c) Gajhede, M. In *Handbook of Metalloproteins*; Messerschmidt, A., Huber, R., Poulos, T. L., Wieghardt, K., Eds.; John-Wiley and Sons: New York, 2001; Vol. 1, pp 193−328. (d) Dawson, J. H.; Sono, M. *Chem. Rev.* **1987**, *87*, 1255−1276. (e) Dawson, J. H. *Science* **1988**, *240*, 433−439. (f) Colas, C.; Ortiz de Montellano, P. R. *Chem. Rev.* **2003**, *103*, 2305−2332. (g) Dunford, H. B. *Heme Peroxidases*; Wiley-VCH: New York, 1999.

(2) Markwalder, H. U.; Neukom, H. *Phytochemistry* **1976**, *15*, 836−837.

10.1021/ja065058d CCC: $33.50

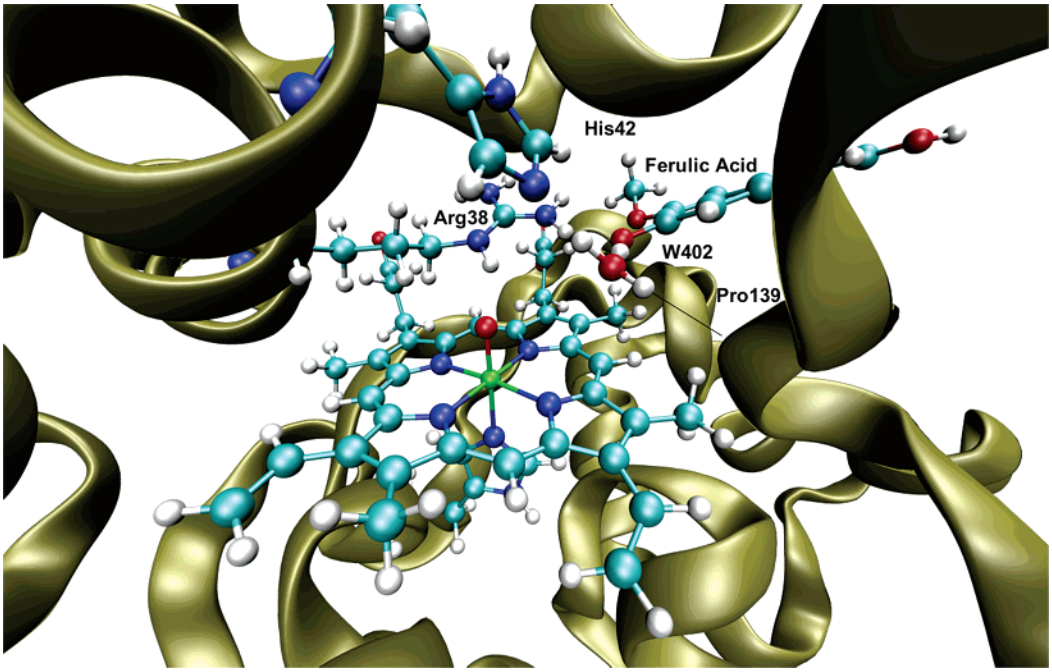

Figure 1. View of the active site of HRP showing the binding mode of ferulic acid with Cpd I (oxo replacing the original water in 6ATJ (PDB code)). A line indicates the hydrogen bond between W402 and Pro139 (not shown explicitly). The residues shown in ball-and-stick format are those calculated at the QM level.

of other questions (see below) are the focus of this paper, which uses hybrid quantum mechanics/molecular mechanics (QM/MM) calculations to investigate the oxidative mechanism of ferulic acid by HRP on a detailed molecular level.

The structure of the HRP resting state with ferulic acid has been solved by X-ray crystallography[4,5] and therefore constitutes a good starting point for studying theoretically the catalytic cycle of HRP. The X-ray structure shows that ferulic acid maintains close contacts with two residues of the active site: Arg38 and His42 (see Figure 1). Moreover, the presence of two water molecules in the active site (one bonded to iron, the second close to Pro139) has been extensively discussed by Gajhede.[4,5] It seems that this second water molecule (W402 in Figure 1) is in a good position to relay protons between the substrate and the oxoiron moiety. If this water molecule plays an important role in the redox processes in peroxidases, it will also explain why Pro139, or a Pro residue in a similar position in other peroxidases, is highly conserved in the family of peroxidases. This is typically a question QM/MM calculations can resolve.

Extensive experiments regarding the kinetics of HRP have been carried out to decipher the species in the catalytic cycle of HRP. On the basis of these works, it appears that HRP oxidizes phenols in a two-step mechanism,[6] involving substrate binding followed by electron and proton transfers. With phenols as substrates, the rate-limiting step for the entire cycle in Scheme 1 is the O−O bond breaking during formation of Cpd I. This means that the oxidation of phenols must be a fast and efficient process. Furthermore, it has also been demonstrated that for a series of substituted phenols (and anilines) there exists a correlation between the rate constants for oxidation and the energy levels of the highest occupied MO (HOMO)[7a] of the substrates. A good correlation was obtained also with Hammett's σ constants of the phenyl substituents but not with the Okamoto−Brown constants,[7a,b] thus strengthening the conclusion that the phenyl ring of the phenol does not actually acquire a positive charge during the reaction, and as such, the mechanism involves coupled electron and proton transfers. This coupled mechanism is interesting considering the facts that the ionization potential of ferulic acid is 176.2 kcal/mol (this work) and the O−H bond energy is significant. So what makes the process so facile? Accordingly, we shall aim to establish by means of QM/MM a precise nature of the oxidative process and of the means whereby the cycle returns to its starting point, the resting state.

In recent papers, we showed by means of QM/MM calculations that the electronic structure of Cpd I is affected by two residues in the active site (Arg38 and His42)[8] and conforms to the well-accepted[9] description of the species with a radical cation porphyrin weakly coupled to the triplet electrons of the Fe═O moiety. Subsequently,[10] we showed that the secondary active species Cpd II is, by contrast, considerably more complex than hitherto appreciated, as noted in a recent review.[11] Some of this

(3) For some general references on PCET mechanisms, see: (a) Cukier, R. I.; Nocera, D. G. *Annu. Rev. Phys. Chem.* **1998**, *49*, 337−339. (b) Stubbe, J.; Nocera, D. G.; Yee, C. S.; Chang, M. C. Y. *Chem. Rev.* **2003**, *103*, 2167−2201. (c) Mayer, J. M. *Annu. Rev. Phys. Chem.* **2005**, *55*, 363−390.
(4) Henriksen, A.; Smith, A. T.; Gajhede, M. *J. Biol. Chem.* **1999**, *274*, 35005−35011.
(5) Gajhede, M. *Biochem. Soc. Trans.* **2001**, *29*, 91−99.
(6) Rodriguez-Lopez, J. N.; Gilabert, M. A.; Tudela, J.; Thorneley, R. N. F.; Garcia-Canovas, F. *Biochemistry* **2000**, *39*, 13201−13209.
(7) (a) Sakurada, J.; Sekiguchi, R.; Sato, K.; Hosoya, T. *Biochemistry* **1990**, *29*, 4093−4098. (b) For a succinct review of the reactivity of phenols and anilines, see ref 1g, pp 75−77, 82−84, and 130−131.
(8) Derat, E.; Cohen, S.; Shaik, S.; Altun, A.; Thiel, W. *J. Am. Chem. Soc.* **2005**, *127*, 13611−13621.
(9) (a) Harris, D. L. *Curr. Opin. Chem. Biol.* **2001**, *5*, 724. (b) Dolphin, D.; Forman, A.; Borg, D. C.; Fajer, J.; Felton, R. H. *Proc. Natl. Acad. Sci. U.S.A.* **1971**, *68*, 614. (c) Dolphin, D.; Felton, R. H. *Acc. Chem. Res.* **1974**, *7*, 26. (d) DiNello, R. K.; Dolphin, D. H. *J. Biol. Chem.* **1981**, *256*, 6903. (e) Schulz, C. E.; Rutter, R.; Sage, J. T.; Debrunner, P. G.; Hager, L. P. *Biochemistry* **1984**, *23*, 4743. (f) Kim, S. H.; Perera, R.; Hager, L. P.; Dawson, J. H.; Hoffman, B. M. *J. Am. Chem. Soc.* **2006**, *128*, 5598−5599. (g). Harvey, J. N.; Bathelt, C. M.; Mulholland, A. J. *J. Comput. Chem.* **2006**, *27*, 1352−1362. (h) Green, M. T. *J. Am. Chem. Soc.* **2000**, *122*, 9495. (i) de Visser, S. P.; Shaik, S.; Sharma, P. K.; Kumar, D.; Thiel, W. *J. Am. Chem. Soc.* **2003**, *125*, 15779. (j) Rydberg, P.; Sigfridsson, E.; Ryde, U. *J. Biol. Inorg. Chem.* **2004**, *9*, 203.

complexity, unraveled by the calculations,[10] is illustrated in Scheme 1 by the multiple isomers of Cpd II (**2**, Scheme 1). Thus, Cpd II has a ferryl isomer, **2a**, and iron−hydroxo isomers **2b** in two different electromers, one with Fe^{III} and a porphyrin radical cation, **2b**(III), and the other with Fe^{IV} and a closed shell porphyrin, **2b**(IV). In addition, there also seems to be an aquairon isomer with Fe^{III} and a porphyrin radical cation, **2b**−H^+(III). This complex picture naturally raises the question of whether all these species, in Scheme 1, participate in the mechanism of ferulic acid oxidation. As we shall demonstrate, Cpd I and two of the isomers of Cpd II participate in the oxidation of ferulic acid and are necessary to close the cycle and return to the resting state. The formation of Cpd I from the ferric complex and H_2O_2 has been treated in a previous paper,[12] where it was found to obey the Poulos−Kraut mechanism,[1b] and it will not be addressed here any further.

The paper has two parts. In the first part, we deal with the oxidation of ferulic acid by Cpd I and try to answer the following questions: What is the precise mechanism of substrate oxidation, ET, PT, H atom transfer, or PCET? What is the driving force for the oxidation of the substrate and the conversion of Cpd I to Cpd II? Does the ferulic acid (FA) substrate have an influence on the electronic and geometrical structure of Cpd I and Cpd II? The second part of this paper addresses the problem of the regeneration of the resting state from Cpd II by means of a second substrate oxidation process and attempts to answer the following questions: Is Cpd II an oxidant as powerful as Cpd I? Which forms of Cpd II are the active ones, and how does the process lead to a full cycle?

Methods

QM/MM Methodology and Software. The QM/MM method[13] dissects the total enzyme into two subsystems: the active center and the rest. The active center is described by a quantum mechanical method, in the present case DFT in the unrestricted Kohn−Sham formalism employing the B3LYP[14] and PBE0[15] functionals. The rest of the system (see below) is treated by molecular mechanics using a force field calibrated for proteins.[16] The two subsystems are allowed to interact by electrostatic and van der Waals terms, such that the QM subsystem adapts its electronic structure and charge distribution from the field exerted by the protein environment. In the present study we apply the electrostatic embedding scheme,[17] which incorporates the MM charges into the one-electron Hamiltonian of the QM procedure, while the dangling bonds at the QM/MM boundary are capped with hydrogen link atoms in the framework of the charge shift method. The Chemshell[18] software is used to perform the QM/MM calculations by integrating the TURBOMOLE package[19] for QM and the DL-POLY program[20] for MM using the CHARMM22 force field.

To be consistent with recent QM/MM studies of Cpd I and Cpd II of HRP,[8,10,12] we used here two basis sets for the QM/MM calculations: for geometry optimization we utilized LACVP, a double-ζ basis set with an effective core potential on iron,[21] hereafter, B1, while for single-point energy calculations we used a larger all-electron basis set, referred to as B2. In B2, iron is described by the Wachters all-electron basis set augmented with diffuse d and f polarization functions,[22] while the immediate coordination spheres of iron and other electronegative atoms are represented by 6-31+G(d) and those of the remaining atoms by 6-31G(d).[23] These single-point energies are labeled as B2//B1. A test of the barrier for PCET was carried out using QM-only calculations with the MPW1K functional developed by Lynch et al.[24] for barriers of H-transfer processes.

Setup of the System. To prepare suitable initial structures for the QM/MM calculations, we started from the experimental X-ray structure of HRP in complex with FA[4] (PDB code 6ATJ) and built a complete model of the solvated enzyme by adding the missing hydrogen atoms and a 16 Å thick water solvent layer. Two models were studied: the first one corresponds to Cpd I with FA and the second to Cpd II with FA. For the oxidative process with Cpd I, the complete system consists of 19282 atoms, including 13293 atoms in the solvent, whereas with Cpd II the system consists of 19274 atoms, including 13284 in the solvent. These systems were subsequently relaxed by performing pure force field energy minimizations and short molecular dynamics (MD) simulations, using the CHARMM22 force field. During these classical force field calculations, the coordinates of the entire heme unit and the coordinated histidine were kept fixed. The MD calculations did not significantly modify the structure compared with the initial X-ray structure. Therefore, we performed the QM/MM calculations on the coordinates obtained after simple force field energy minimizations and short MD on the inner solvent layer (done to remove close contacts).

Charged Residues and Total Charge of the System. The total charges of the so-generated Cpd I and Cpd II systems were zero and corresponded to the following protonated state of the various residues: Aspartates (Asp) and glutamates (Glu) were used as negatively charged (Asp8, Asp20, Asp29, Asp43, Asp50, Asp56, Asp81, Asp66, Asp99, Asp125, Asp132, Asp150, Asp162, Asp182, Asp194, Asp220, Asp222, Asp230, Asp247, Asp258, Asp282; Glu25, Glu64, Glu88, Glu238, Glu239, Glu249, Glu279), and arginines (Arg) and lysines (Lys) were used as positively charged (Arg19, Arg27, Arg31, Arg38, Arg62, Arg75, Arg82, Arg93, Arg118, Arg123, Arg124, Arg153, Arg159, Arg178, Arg183, Arg206, Arg224, Arg264, Arg283, Arg298, Arg302; Lys65, Lys84, Lys149, Lys174, Lys232, Lys241). One more positive charge is "located" on the heme moiety. The histidines (His40, His42, His170) were singly protonated and hence electrically neutral. Of these His residues, one is the proximal ligand, His170, and the other is the distal residue, His42, which was kept neutral to initiate the process (it will become protonated during the process).

QM Region. On the basis of a previous study of Cpd I (see Figure 1), using the same methodology, the mechanism was investigated using a QM subsystem comprising the heme with its distal ligand (O or OH) and proximal ligand (modeled as an imidazole), Arg38, His42, W402, and ferulic acid.

(10) Derat, E.; Shaik, S. *J. Am. Chem. Soc.* **2006**, *128*, 8185−8198.
(11) Andersson, L. A.; Dawson, J. H. *Struct. Bonding (Berlin)* **1990**, *74*, 1−40.
(12) Derat, E.; Shaik, S. *J. Phys. Chem. B* **2006**, *110*, 10526−10533.
(13) For a small selection of reviews, see: (a) Aqvist, J.; Warshel, *A. Chem. Rev.* **1993**, *93*, 2523−2544. (b) Gao, J. In *Reviews in Computational Chemistry*; Lipkowitz, K. B., Boyd, D. B., Eds.; VCH: Weinheim, Germany, 1995; Vol. 7, p 119. (c) Mordasini, T. Z.; Thiel, W. *Chimia* **1998**, *52*, 288−291. (d) Monard, G.; Merz, K. M., Jr. *Acc. Chem. Res*. **1999**, *32*, 904−911. (e) Sherwood, P. In *Modern Methods and Algorithms of Quantum Chemistry*; Grotendorst, J., Ed.; NIC Series 3; John von Neumann Institute for Computing: Jülich, Germany, 2000; p 285. (f) Gao, J.; Truhlar, D. G. *Annu. Rev. Phys. Chem.* **2002**, *53*, 467−505. (g) Field, M. J. *J. Comput. Chem.* **2002**, *23*, 48−58. (h) Monard, G.; Prat-Resina, X.; Gonzalez-Lafont, A.; Lluch, J. M. *Int. J. Quantum Chem.* **2003**, *93*, 229−244. (i) Ridder, L.; Mulholland, A. *Curr. Top. Med. Chem.* **2003**, *3*, 1241−1256.
(14) (a) Becke, A. D. *Phys. Rev. A* **1988**, *36*, 3098−3100. (b) Lee, C.; Yang, W.; Parr, R. G. *Phys. Rev. B* **1988**, *37*, 785−789. (c) Becke, A. D. *J. Chem. Phys.* **1993**, *98*, 5648−5652.
(15) (a) Perdew, J. P.; Burke, K.; Ernzerhof, M. *Phys. Rev. Lett.* **1996**, *77*, 3865−3868. (b) Perdew, J. P.; Ernzerhof, M.; Burke, K. *J. Chem. Phys.* **1996**, *105*, 9982−9985.
(16) MacKerell, A. D., Jr.; et al. *J. Phys. Chem. B* **1998**, *102*, 3586−3616.
(17) Bakowies, D.; Thiel, W. *J. Phys. Chem.* **1996**, *100*, 10580−10594.
(18) Sherwood, P.; et al. *J. Mol. Struct.: THEOCHEM* **2003**, *632*, 1−28.
(19) Ahlrichs, R.; Bär, M.; Häser, M.; Horn, H.; Kölmel, C. *Chem. Phys. Lett.* **1989**, *162*, 165−169.
(20) Smith, W.; Forester, T. *J. Mol. Graphics* **1996**, *14*, 136−141.
(21) LACVP is constructed from the LANL2DZ basis sets: (a) Hay, J. P.; Wadt, W. R. *J. Chem. Phys.* **1985**, *82*, 299−310. (b) Friesner, R. A.; Murphy, R. B.; Beachy, M. D.; Ringlanda, M. N.; Pollard, W. T.; Dunietz, B. D.; Cao, Y. X. *J. Phys. Chem. A* **1999**, *103*, 1913−1928.
(22) Wachters, A. J. H. *J. Chem. Phys.* **1970**, *52*, 1033−1036.
(23) Hehre, W. J.; Ditchfield, R.; Pople, J. A. *J. Chem. Phys.* **1972**, *56*, 2257−2261.
(24) Lynch, B. J.; Fast, P. L.; Harris, M.; Truhlar, D. G. *J. Phys. Chem. A* **2000**, *104*, 4811−4815.

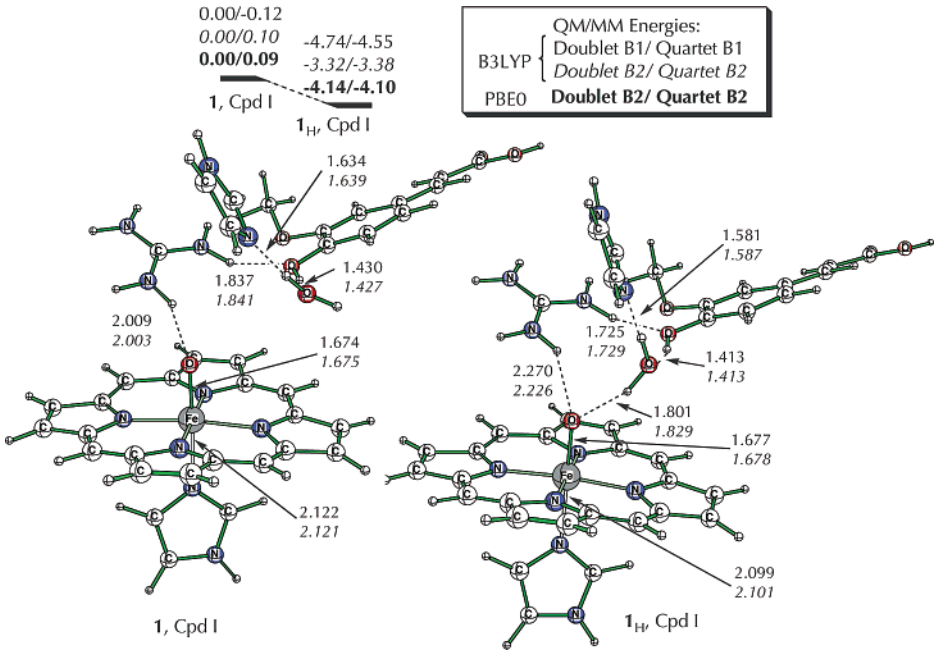

Figure 2. Reorganization of the hydrogen bonding network in the active site of Cpd I with FA. Geometries are obtained at the QM(UB3LYP/B1):MM-(CHARMM) level. Distances are in angstroms and correspond to the doublet state, in regular font, or to the quartet state, in italics. In **1**, W402 is linked to Pro139 (not shown), whereas in $\mathbf{1}_H$, there is a hydrogen bond with the oxo group of Cpd I.

Optimized QM/MM Region. The QM/MM geometry optimization includes the following residues: Arg31, Ser35, Arg38, Phe41, His42, Phe68, Gly69, Asn70, Ser73, Leu138, Pro139, Ala140, Pro141, Phe142, Ser167, His170 (including the heme), Gln176, Phe179, Ile244, Asp247, Phe221, Tyr233, ferulic acid, W4, W55, W72, W143, W217, W238, W267, W275, W402.

The data generated for this study are summarized in the Supporting Information (SI). Key data are discussed in the following text.

Results

Oxidation of Ferulic Acid by Cpd I. The optimized structure of Cpd I in the presence of FA is shown in Figure 2 and is labeled as **1**. Most of the bond lengths within Cpd I are very similar to those found before[12] without the presence of FA and in the presence of a neutral His42 residue. The crucial structural element is the water molecule W402, which forms hydrogen bonds (H-bonds) with Pro139 and His42, but is not oriented favorably to relay protons from the FA substrate to Cpd I. Therefore, a preorganization step must precede the oxidation of the FA. This preorganized structure, labeled as $\mathbf{1}_H$, is shown on the right-hand side of Figure 2. It is seen that the W402 molecule is engaged in three H-bonds, one to the phenolic proton of FA (distance 1.413 Å), one to His42, and one to the oxo group of Cpd I. This is a perfect setup for transfer of protons between FA and Cpd I. Furthermore, it is apparent that the new architecture $\mathbf{1}_H$ is stabilized relative to the unorganized structure **1** by a significant amount with the two basis sets and the two functionals.

Figure 3 depicts the mechanism of FA oxidation starting from $\mathbf{1}_H$; FA is labeled here as ArOH. The geometric details of the key species are given in Figures 4 and 5; the intermediates are shown in Figure 4 and the TSs in Figure 5. Initially, Figure 3 shows that the substrate loses, via **TS1**, the phenolic hydrogen to His42, which becomes His42$-H^+$, the FA is converted to an ArO$^\bullet$ radical, and Cpd I becomes Cpd II in its oxoferryl **2a** isomer. At the same time W402 rearranges to maintain H-bonding with the ArO$^\bullet$ species and the protonated His42$-H^+$ (see **2a** in Figure 4). As such, this initial step involves transfers of a proton from ArOH to one location (His42) and an electron to another location (the porphyrin radical cation of Cpd I, $\mathbf{1}_H$). Since these two events occur in a single step, the oxidation step is a PCET step,[3] in accord with conclusions based on experimental investigations.[4,5,7] The barrier for this step is seen to be 6.1−6.7 and 6.5−6.9 kcal/mol for the doublet and quartet states, respectively, of Cpd I at the highest level (B2//B1) for the two functionals. A test with the MPW1K functional,[24] using QM-only calculations (done without point charges for technical reasons) increases the barrier by 4.7 kcal/mol (B1 basis set). Using the experimental rate constant,[4] the free energy barrier at room temperature is 8.6 kcal/mol. Thus, the three functionals give reasonable estimates of the barrier, 6−11 kcal/mol, compared with 8.6 kcal/mol in the experiment. This is a very low barrier indicating a fast and efficient process, at least by comparison to other barriers of H-transfer with B3LYP.[25]

Following the oxidation of ferulic acid and formation of the intermediate **2a/(**ArO$^\bullet$, His42$-H^+$, W402), there occur a series of PT reactions with extremely low barriers which give the aqua−ferric Cpd II isomer **2b**$-H^+$(III).[10] Initially, the protonated His42 relays its excess proton to the oxo group of **2a** via **TS2** and generates the **2b**(IV) isomer of Cpd II. The latter is converted to the more stable isomer **2b**(III),[10] which in turn abstracts a proton from Arg38 to form **2b**$-H^+$(III). This latter species is interesting, since it is formed easily in the presence of the ArO$^\bullet$ radical but collapses back to **2b**(III) in the presence of a fresh FA substrate (see Figure SI1 in the SI). This is a result of **2b**$-H^+$(III) being highly unstable compared to the **2b**(III) isomer in the presence of FA (Figure SI1). This change in the stability of the **2b**$-H^+$(III) isomer of Cpd II may be meaningful, *although we cannot state with confidence that it is*

(25) de Visser, S. P.; Kumar, D.; Cohen, S.; Shacham, R.; Shaik, S. *J. Am. Chem. Soc.* **2004**, *126*, 8362−8363.

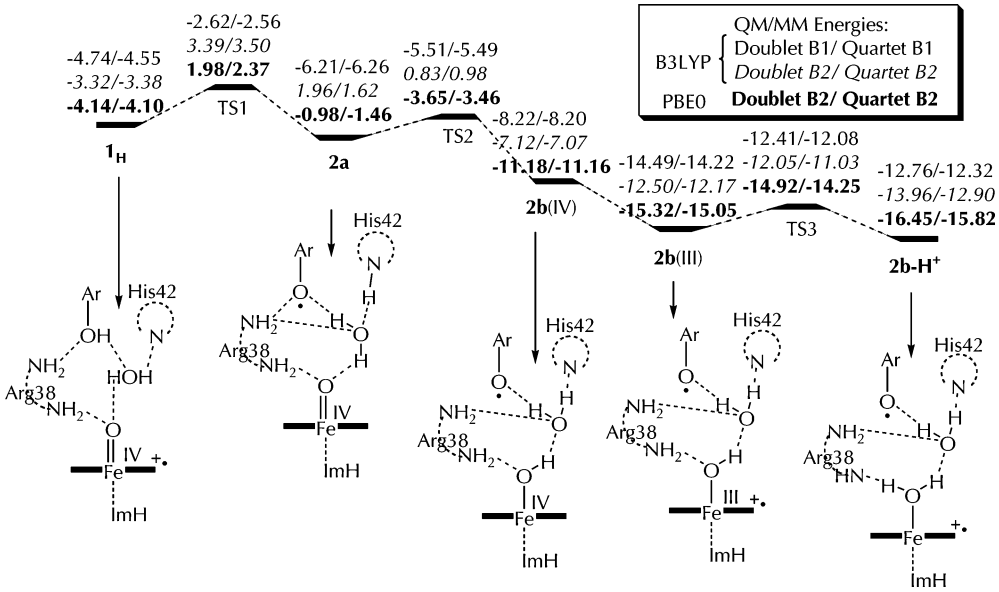

Figure 3. Energy profile for the PCET between compound I and ferulic acid (ArOH) leading to compound II. Data are given with two functionals (B3LYP and PBE0) and two basis sets (B1 and B2) and are in kilocalories per mole.

not an artificial feature of the QM/MM calculations, since Arg38 is a rather poor acid. As we argued before,[10] the deprotonated Arg38 may be just a short-lived species that will instantly regain its normal state by protons from the surface of the protein. In this qualified sense, **2b**−H^+(III) might well be a new real species of Cpd II,[26] and as noted before,[10] it offers the most likely rationale for the observation that Cpd II of HRP exchanges water with the surroundings in the presence of $H_2{}^{18}O$.[27]

The geometries of the key intermediates in the above mechanism are shown in Figure 4; the structures of the Cpd II intermediates are similar to those already reported by HRP.[10] The new feature here is the H-bond network that is generated by W402 and which continues to connect all the key groups that participate in this mechanism, through PCET followed by successive PT events. The transition-state geometries for this mechanism are collected in Figure 5 and reveal the crucial role of W402. Thus, **TS1** shows clearly how the ferulic acid oxidation is mediated by W402, which abstracts the phenolic proton and at the same time transfers a proton to His42; as discussed later the ferulic acid also loses an electron that "sinks" into the porphyrin hole of Cpd I. **TS2** shows that, once again, the proton transfer from His42−H^+ to the iron−oxo species of **2a** is mediated by W402. The last transition state, **TS3**, shows the last PT event from Arg38 to **2b**(III) to generate the final aqua−ferric intermediate of Cpd II.

Finally, a notable feature of the mechanism in Figure 3 is that the entire energy profile is in fact doubled due to the proximity of the doublet and quartet spin states throughout the mechanism, a feature referred to as two-state reactivity (TSR).[28,29] In view of the recent finding about magnetic field effects on the reaction of HRP, the TSR feature may or may not be

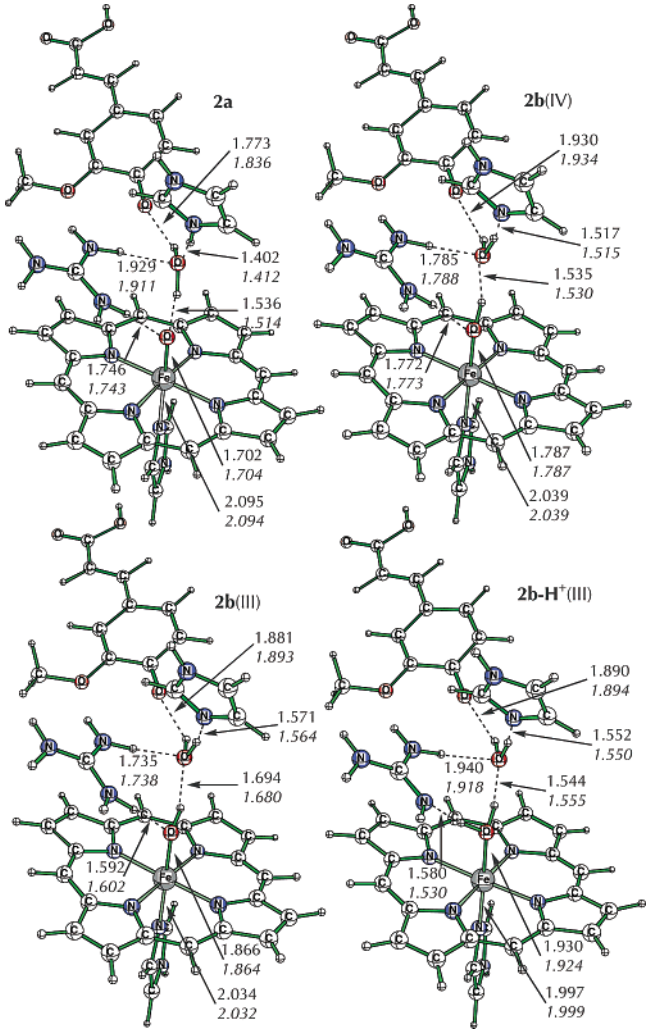

Figure 4. Structures of the intermediates between Cpd I and Cpd II in interaction with FA at the QM(UB3LYP/B1):MM(CHARMM) level. Distances are in angstroms and correspond to the doublet state or to the quartet state, in italics.

(26) Note that the Fe−O bond length in **2b**−H^+(III) is almost identical to that of the long-bond species observed in one of the EXAFS experiments; see: (a) Chance, B.; Powers, L.; Ching, Y.; Poulos, T.; Schonbaum, G. R.; Yamazaki, I.; Paul, K. G. *Arch. Biochem. Biophys.* **1984**, *235*, 596−611. (b) Chance, M.; Powers, L.; Poulos, T.; Chance, B. *Biochemistry* **1986**, *25*, 1266−1270.

(27) Hashimoto, S.; Tatsuno, Y.; Kitagawa, T. *Proc. Natl. Acad. Sci. U.S.A.* **1986**, *83*, 2417−2421.

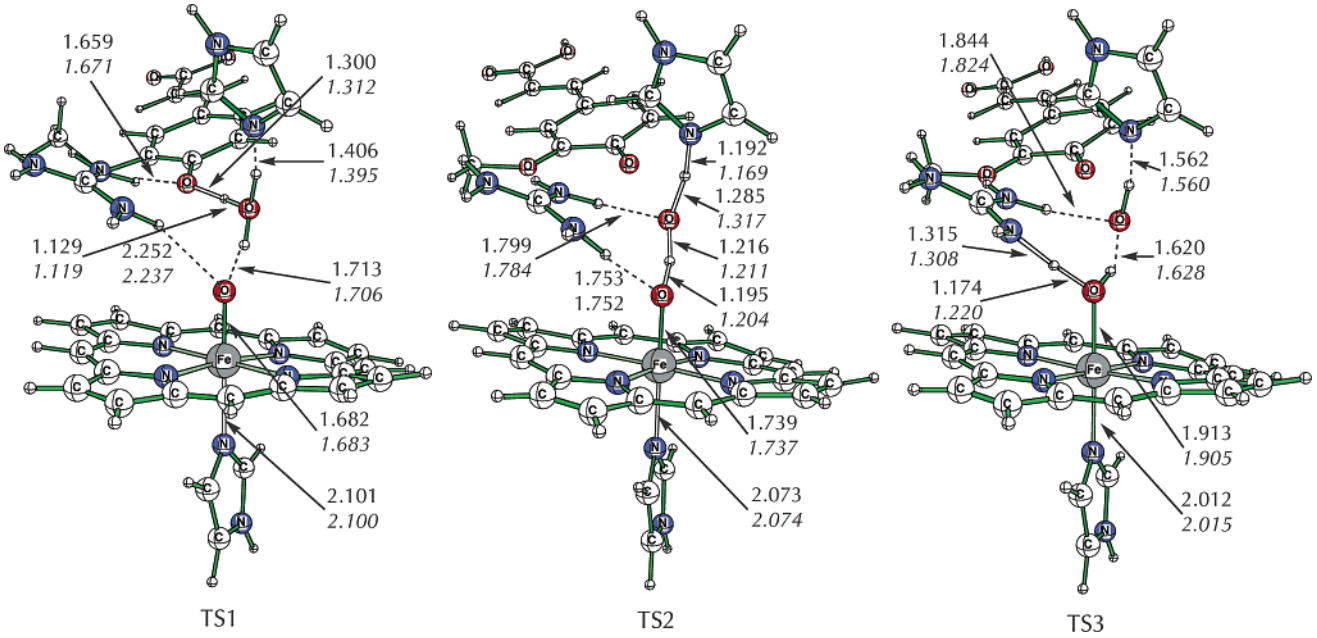

Figure 5. Structures of the transition states for FA oxidation by Cpd I, via the mechanism outlined in Figure 3. **TS1** is the species for the PCET step. Distances, at the QM(UB3LYP/B1):MM(CHARMM) level, are in angstroms and correspond to the doublet state or to the quartet state, in italics.

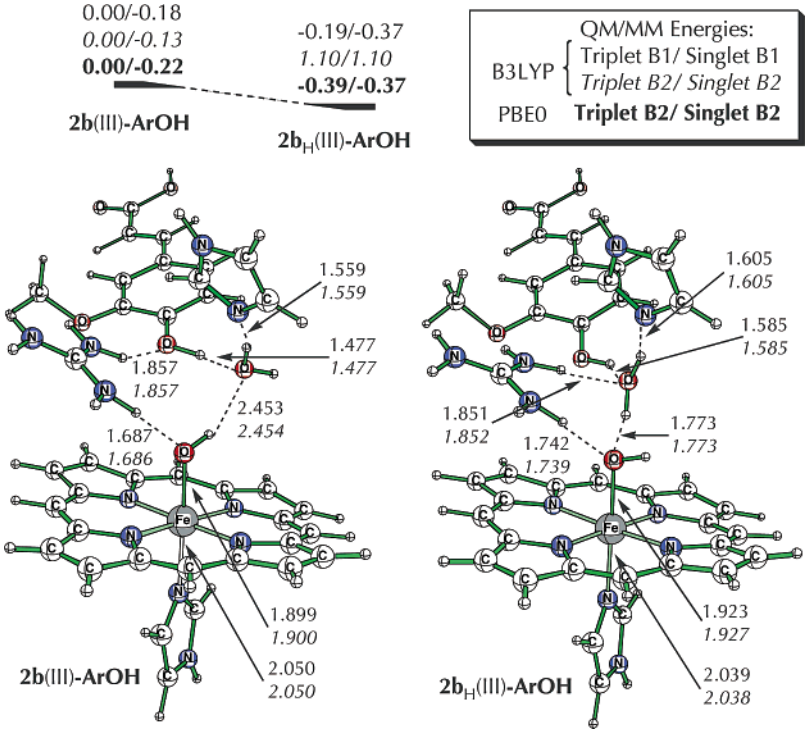

Figure 6. Reorganization of the hydrogen network in the active site of Cpd II. In **2b**(III), W402 is linked to Pro139, whereas in **2b**$_H$(III), there is a hydrogen bond with the hydroxo group. Geometries are obtained at the QM(UB3LYP/B1):MM(CHARMM) level. Distances are in angstroms and correspond to the triplet state or to the open shell singlet state, in italics.

detectable,[30] depending on the strength of the spin−orbit coupling interaction between the states.[31]

Oxidation of Ferulic Acid by Cpd II. As we already noted, the **2b**−H$^+$(III) isomer of Cpd II (see Figure 3) is stable only in the presence of the ArO$^\bullet$ radical derived from FA. In the presence of a fresh FA molecule it collapses spontaneously to the **2b**(III) isomer (see Figure SI1), the latter becoming the ground state of Cpd II. As such, the natural starting point of

(28) (a) Shaik, S.; Danovich, D.; Fiedler, A.; Schröder, D.; Schwarz, H. *Helv. Chim. Acta* **1995**, *78*, 1393−1407. (b) Shaik, S.; Filatov, M.; Schröder, D.; Schwarz, H. *Chem.−Eur. J.* **1998**, *4*, 193−199. (c) Schroeder, D.; Shaik, S.; Schwarz, H. *Acc. Chem. Res.* **2000**, *33*, 139−145. (d) Shaik, S.; de Visser, S. P.; Ogliaro, F.; Schwarz, H.; Schroeder, D. *Curr. Opin. Chem. Biol.* **2002**, *6*, 556−567. (e) Shaik, S.; de Visser, S. P.; Kumar, D.; Altun, A.; Thiel, W. *Chem. Rev.* **2005**, *105*, 2279−2328.

(29) For reviews projecting the generality of TSR, see: (a) Poli, R.; Smith, K. M.; Harvey, J. N. *Coord. Chem. Rev.* **2003**, *238*−*239*, 347−361. (b) Schwarz, H. *Int. J. Mass Spectrom.* **2004**, *237*, 75−105.

(30) (a) Afanasyeva, M. S.; Taraban, M. B.; Purtov, P. A.; Leshina, T. V.; Grissom, C. B. *J. Am. Chem. Soc.* **2006**, *128*, 8651−8658. (b) Jones, A. R.; Scrutton, N. S.; Woodward, J. R. *J. Am. Chem. Soc.* **2006**, *128*, 8408−8409.

(31) Danovich. D.; Shaik, S. *J. Am. Chem. Soc.* **1997**, *119*, 1773−1786.

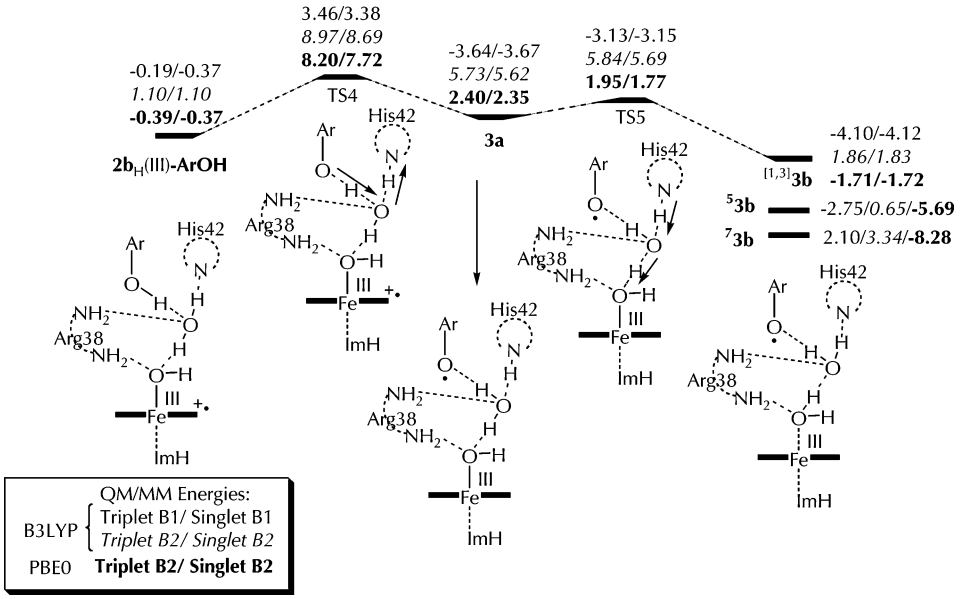

Figure 7. Energy profile for the PCET between Cpd II and FA leading to the resting state. Data are given with two functionals (B3LYP and PBE0) and two basis sets (B1 and B2).

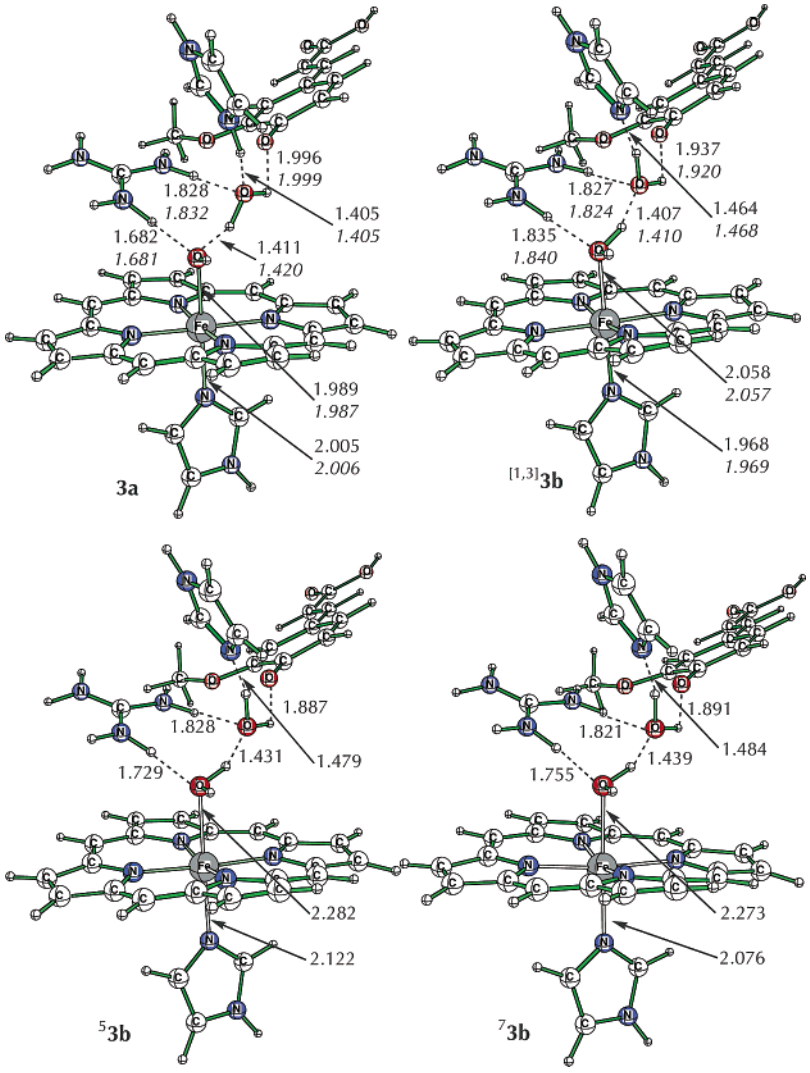

Figure 8. Structures of the intermediates that result from the oxidation of FA by Cpd II (see Figure 7) at the QM(UB3LYP/B1):MM(CHARMM) level. Distances are in angstroms and correspond to the triplet state or to the open shell singlet state, in italics. Also shown are the two high-spin states, ^{5,7}**3b**.

the second oxidative process is **2b**(III) and a freshly incoming FA molecule. Figure 6 shows **2b**(III) in the presence of a new FA molecule. Once again, the W402 is wrongly disposed after the MD, but a preorganization step brings this water molecule

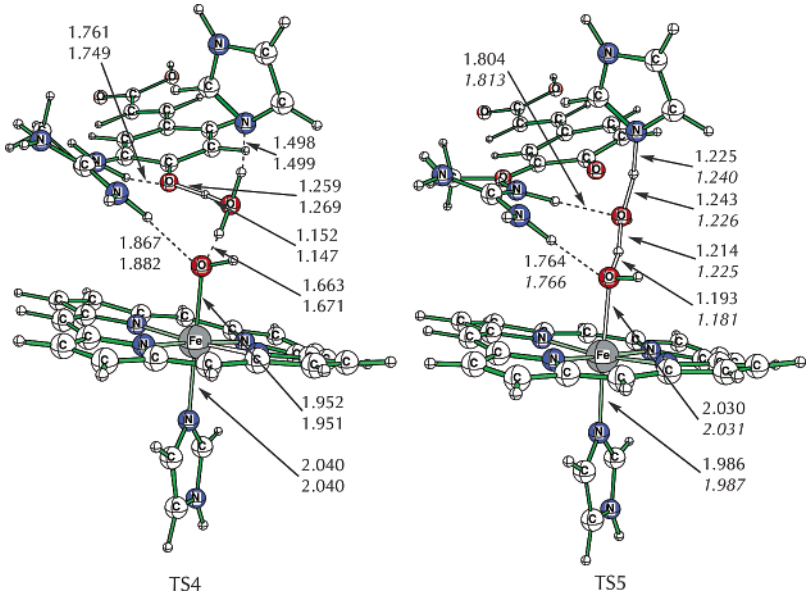

Figure 9. Structures of the transition state during the oxidation of FA by Cpd II (see Figure 7) at the QM(UB3LYP/B1):MM(CHARMM) level. Distances are in angstroms and correspond to the triplet state or to the open shell singlet state, in italics. **TS4** is the species for the PCET step in Figure 7.

Scheme 2. PCET Mechanisms of Oxidation of Ferulic Acid by Cpd I (A–C) and Cpd II (D–F)

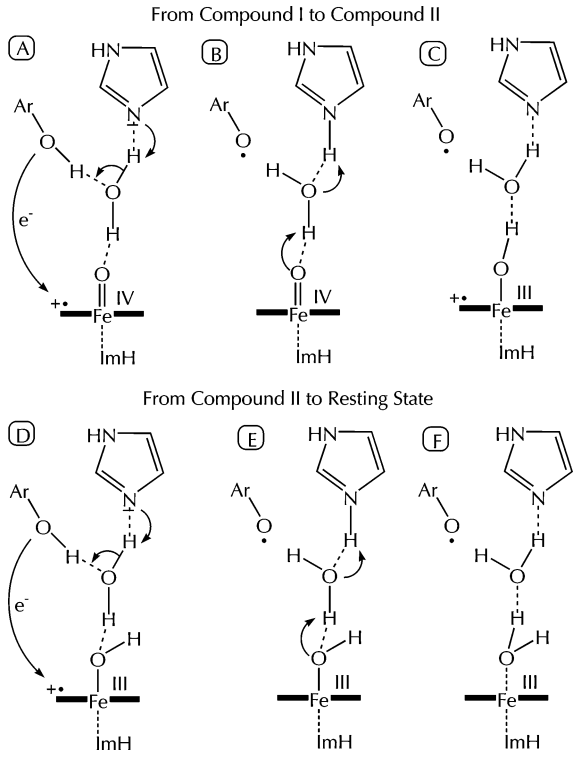

into H-bonding with the FeOH moiety of **2b**(III) to form the **2b**$_H$(III) conformer, which is ready for FA oxidation. Interestingly, FA causes some elongation of the Fe–OH bond in these **2b**(III) and **2b**$_H$(III) species compared with the same **2b**(III) species in the presence of the ArO• radical (Figure 4).

Figure 7 shows the oxidation mechanism starting with **2b**$_H$-(III). In the first step, by complete analogy to the mechanism in Figure 3 above, there is a PCET whereby the ferulic acid (ArOH) loses a proton to His42 and an electron to the porphyrin radical cation moiety of **2b**$_H$(III). This process results in the ferric–hydroxo complex **3a** and the ArO• radical of the oxidized FA. Subsequently, His42–H$^+$ relays its excess proton to the FeOH moiety to generate the aqua–ferric complex **3b**, which is the resting state of the HRP enzyme, thus coming full cycle. Since Cpd II is initially in a triplet or open shell singlet state, the complexes **3a** and **3b** involve doublet FeOH and $FeOH_2$ complexes and radical ArO•. Thus, this Fe^{III}/ArO• radical pair is coupled to give an overall triplet or open shell singlet spin state. Of course, the ground state of **3b** is known to correspond to a pentacoordinated ferric complex (the water ligand is far away, e.g., 3.0 Å in 6ATJ (PDB code)) in a sextet spin state.[32] Our calculations show that the ground state in the presence of ArO• is indeed the sextet heme complex, which together with the radical derived from FA gives rise to the ^{5,7}**2b** states shown in Figure 7.

Figure 8 shows the geometric details of the intermediates in the mechanism described in Figure 7, while Figure 9 shows the corresponding TS geometries. The structure of the intermediate **2b**$_H$(III)–ArOH is similar to that already reported for HRP.[10] The new structures are the ferric–hydroxo **3a** complex and the resting state **3b**, which have geometric characteristics expected from these complexes. Note that, for **3b** in addition to the low-spin doublet species ^{1,3}**3b**, we also show the two high-spin states ^{5,7}**3b**. In the latter complexes, Fe is hexacoordinated. We think that the presence of the FA-derived radical prevents the Fe–OH_2 dissociation, but this may change once the radical leaves the pocket of the enzyme. Since our QM/MM calculations do not allow a dynamic view of the process, this idea cannot be tested.

As before, here too, W402 generates a H-bond network that continues to connect all the key groups that participate in this mechanism of PCET followed by successive PT events. The transition-state geometries in Figure 9 reveal the crucial role of W402 in PCET. Thus, **TS4** shows clearly how the oxidation of FA is mediated by W402, which abstracts the phenolic proton and at the same time transfers a proton to His42; the ferulic acid in turn loses an electron that sinks into the porphyrin hole of Cpd II. **TS5** shows that, once again, the proton transfer from His42–H$^+$ to the iron–hydroxo species **3a** is mediated by

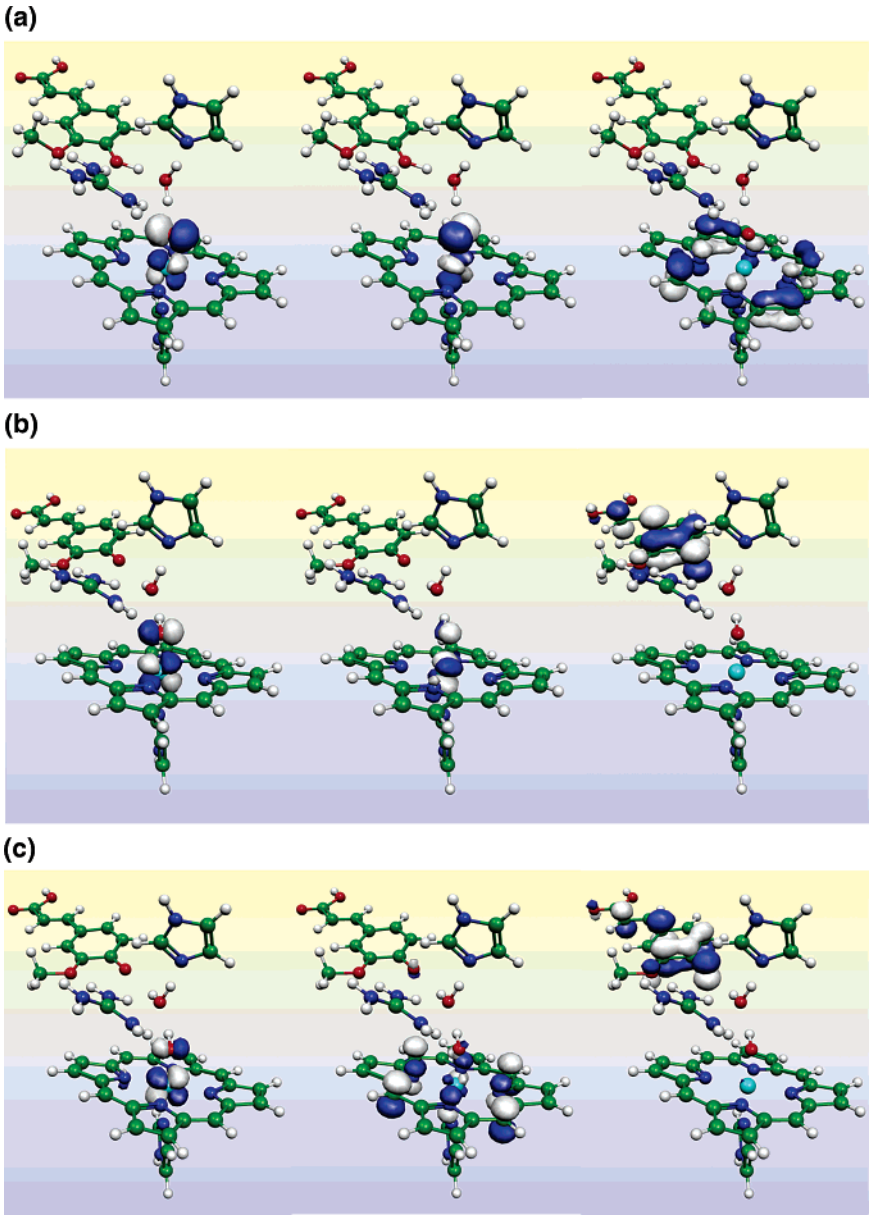

Figure 10. Singly occupied natural orbitals (SONOs) for the three main intermediates in FA oxidation by Cpd I, calculated at the QM(B3LYP/B1):MM-(CHARMM) level: (a) SONOs of Cpd I; (b) SONOs of Cpd II ($Fe^{IV}OH$, **2b**(IV)); (c) SONOs of Cpd II ($Por^{\bullet+}Fe^{III}OH$, **2b**(III)).

W402, which takes up this proton while transferring one to the hydroxo group to generate the resting state.

All in all, we see here similarities to the mechanism of Cpd I. The barrier for the PCET step of Cpd II is 7.9−8.6 kcal/mol, slightly higher than the barrier with Cpd I, but there is no great difference. These barriers can be compared to the free energy barrier, ∼9 kcal/mol, estimated from the experimental rate constant at room temperature.[4] Thus, in accord with experiment, Cpd I is only slightly (4 times) more reactive than Cpd II toward FA oxidation. Another similarity is the degeneracy of the spin states, which doubles the potential energy profile in Figure 7, and hence TSR,[27−29] and the appearance of the higher spin states, which should become accessible by surface crossing en route to the resting state.

Discussion

The mechanisms in Figures 3 and 7 project the critical mechanistic roles of the His42 residue and the water molecule W402. The PCET mechanism is in a way stepwise and mediated by both entities, as depicted schematically by the arrows in Scheme 2 and by the singly occupied orbitals in Figure 10. Thus, starting from the Cpd I species $\mathbf{1}_H$ in Scheme 2A, initially the water relays a proton from the phenol to the His42, while an electron from the OH moiety undergoing deprotonation sinks into the singly occupied porphyrin a_{2u} orbital to produce **2a**, the oxo−ferryl isomer of Cpd II in Scheme 2B. Thus, the PCET step has a few partners; the acid−base partners are the FA−W402−His42 triad, and the electron-transfer partners are the FA (undergoing deprotonation) and the electron-accepting partner Cpd I. Only in the following step (Scheme 2, B → C) the proton ends up on Cpd II (**2a**), leading first to the **2b**(IV) hydroxo−ferryl isomer and then by internal conversion to the more stable **2b**(III) isomer.[10] Thus, it is only during this step (B → C), when the active species of HRP become basic enough (Cpd II **2a** is

(32) (a) Reference 1g, pp 196−198. (b) Maltempo, M. M.; Ohlsson, P.-I.; Petersson, P. L.; Ehrenberg, A. *Biochemistry* **1979**, *18*, 2395−2341. (c) Kobayashi, K.; Tamura, M.; Koichiro, H.; Hori, H.; Morimoto, H. *J. Biol. Chem.* **1980**, *255*, 2239−2242.

more basic[33] than Cpd I), that it can then join the acid−base partners, and the proton is relayed thought the His42−H^+/W402/Cpd II (**2a**) triad.

The electron occupation changes in Figure 10 reveal the same information. Initially in panel a we can see the three singly occupied orbitals of Cpd I,[8,9] two π*(FeO) orbitals and one a_{2u} orbital. In panel b we see the orbitals after the PCET, two π*(FeO) orbitals belonging to the oxo−ferryl **2b**(IV) isomer of Cpd II and a third one now localized on the FA radical. Finally, in panel c, we see the internal conversion to the **2b**(III) isomer, where the two singly occupied orbitals of Cpd II are one of the former π*(FeO) orbitals and the a_{2u}-type orbital and the third one is still localized on the FA radical.

Following the internal conversion of Cpd II to the **2b**(III) isomer, we have a restart of a new PCET mechanism, shown in Scheme 2D. Thus, the acid−base partners, in the FA−W402−His42 triad, transfer a proton to His42, while an electron from FA undergoing deprotonation sinks into the a_{2u} hole of the **2b**(III) isomer of Cpd II. Since the species $Fe^{III}OH$ is now a better base after accepting an electron, it joins the acid−base partners and accepts a proton from His42−H^+ by relay through W402.

The importance of the **2b**(III) isomer of Cpd II is apparent from the comparison of the barriers in Figures 3 and 7. The barriers for Cpd I and Cpd II are seen to be rather similar, the one for Cpd I being slightly lower, as indicated also by the experimental rate constant data, which show a 4-fold difference in reactivity.[4] The rationale for this is quite simple; in both Cpd I and the **2b**(III) isomer of Cpd II the electron-accepting orbital is the porphyrin a_{2u} hole (compare panels a and c in Figure 10). Therefore, Cpd II (**2b**(III)) is almost as good an electron acceptor as Cpd I. Since the proton-transfer part of the PCET does not involve the Cpd I or Cpd II moieties, the two active species participate as ET partners only, and the barriers for the PCET processes are similar. Of course, if Cpd II were to utilize the **2b**(IV) isomer in the substrate oxidation, we would have expected more pronounced differences, making Cpd II significantly less reactive than Cpd I compared to what we find here and to experimental data. It appears that, in many cases of phenol and amine oxidations, Cpd I is indeed significantly more reactive compared with Cpd II.[7,34] Our results do not allow us to decide when we might expect the **2b**(IV) isomer to react instead of the **2b**(III) isomer. This may depend on the substrate, as hinted by our observation that **2b**−H^+(III) is destabilized in the presence of fresh FA. This however is the subject of further investigations.

Another aspect is the TSR, which typifies both mechanisms, due to the near degeneracy of the two states nascent from the initial doublet and quartet states of Cpd I. In the mechanism of Cpd II (Figure 7), there are two additional states and a step of spin crossover will be required to reach the ground state of the resting state. The recent reports on magnetic field effects[30] in HRP suggest that the TSR scenario may be manipulated by magnetic fields, especially for the states near degeneracy in Figures 3 and 7.

Scheme 3. Catalytic Cycle of HRP in the Presence of a Phenolic Substrate Based on the QM/MM Computational Data

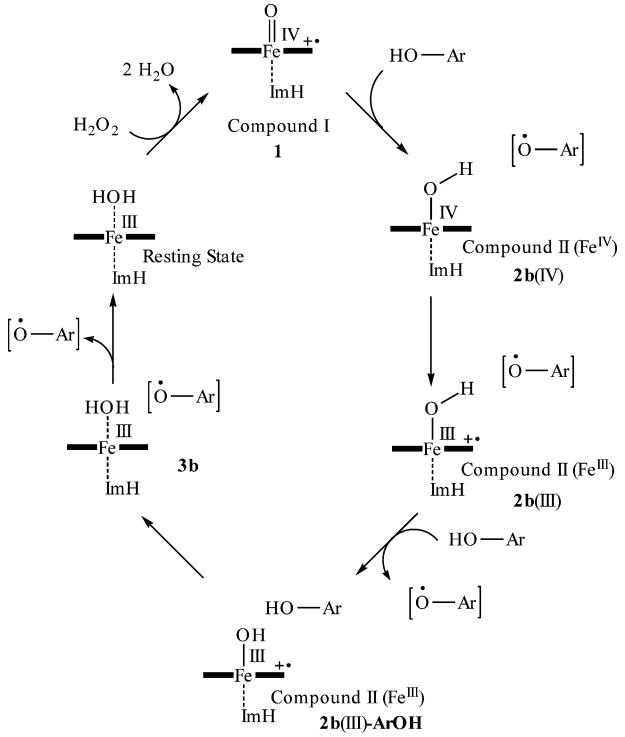

Conclusions

Scheme 3 summarizes a short-hand version of the final catalytic cycle of HRP in the presence of FA based on the QM/MM results in Figures 3 and 7. The PCET mechanism involves deprotonation of FA by the His42−W402 pair and simultaneous electron transfer from the FA undergoing deprotonation to the porphyrin radical cation in the active species. Initially, this forms the **2a** isomer of CpdII (Figure 3), which is converted to **2b**(IV) by proton relay from the protonated His42.

The above PCET mechanism shows that *His42 and W402 are crucial moieties*; *they determine the function of the HRP enzyme* and account for its ability to perform substrate oxidation. The effects of His42 and W402 are well recognized and have been discussed before by Gajhede et al.,[4,5] albeit not with the molecular details available here via the QM/MM computations. On the other hand, the role of Arg38 is less apparent from the calculations, and other than its field effect due to the positive charge that may facilitate the electron-transfer aspect from the FA undergoing deprotonation to Cpd I and Cpd II, and also maintainance of the hydrogen bond network in the active site, we cannot see a more active role.

The possibility of manipulating substrate oxidation by magnetic fields is an intriguing possibility.

Acknowledgment. This research was supported in part by the German Federal Ministry of Education and Research (BMBF) within the framework of the German-Israeli Project Cooperation (DIP) and by an ISF grant.

Supporting Information Available: Ten tables, one figure, *xyz* coordinates of QM regions for all the systems, and refs 16 and 18 in full. This material is available free of charge via the Internet at http://pubs.acs.org.

JA065058D

(33) Green, M. T.; Dawson, J. H.; Gray H. B. *Science* **2004**, *304*, 1653−1656.
(34) For a few additional sources on the reactivity of HRP, see: (a) Candeias, L. P.; Folkes, L. K.; Porssa, M.; Parrick, J.; Wardman, P. *Biochemistry* **1996**, *35*, 102−108. (b) Laurenti, E.; Ghibaudi, E.; Ardissone, S.; Ferrari, R. P. *J. Inorg. Biochem.* **2003**, *95*, 171−176. (c) Candeias, L. P.; Folkes, L. K.; Porssa, M.; Wardman, P. *Biochemistry* **1997**, *36*, 7081−7085. (d) Gilabert, M. A.; Hiner, A. N. P.; Garcia-Ruiz, P. A.; Tudela, J.; Garcia-Molina, F.; Acosta, M.; Garcia-Canovas, F.; Rodriguez-Lopez, J. N. *Biochim. Biophys. Acta* **2004**, *1699*, 235−243.